J Comput Aided Mol Des (2012) 26:983–992
DOI 10.1007/s10822-012-9593-7

Identification of common inhibitors of wild-type and T315I mutant of BCR-ABL through the parallel structure-based virtual screening

Hwangseo Park · Seunghee Hong · Sungwoo Hong

Received: 30 January 2012 / Accepted: 6 August 2012 / Published online: 11 August 2012

Abstract Although the constitutively activated breakpoint cluster region-Abelson (BCR-ABL) tyrosine kinase was well known to be responsible for chronic myelogenous leukemia (CML), the existence of drug-resistant mutants of BCR-ABL has made it difficult to develop effective anti-CML drugs. Here, we report the first example for a successful application of the structure-based virtual screening to identify two common inhibitors equipotent for the wild type and the most drug-resistant T315I mutant of BCR-ABL. Because both inhibitors were screened for having desirable physicochemical properties as a drug candidate and revealed micromolar inhibitory activities, they deserve consideration for further development by structure–activity relationship (SAR) studies to optimize the anti-CML activity. We also address the structural features relevant to the stabilizations of the identified inhibitors in the ATP-binding sites. The results indicate that the inhibitors should be less stabilized by the hydrogen-bond interactions with the change of the receptor from the wild type to T315I mutant due to the replacement of the hydroxy group with the ethyl moiety in the ATP-binding site. Nonetheless, the inhibitors are found to be capable of maintaining the potency for the mutant through the strengthening of hydrophobic interactions to the extent sufficient to compensate for the loss of some hydrogen bonds. This differential binding mode may serve as key information for designing new common inhibitors of the wild type and T315I mutant of BCR-ABL.

Keywords Virtual screening · Drug discovery · Docking · BCR-ABL · Common inhibitor

Electronic supplementary material The online version of this article (doi:10.1007/s10822-012-9593-7) contains supplementary material, which is available to authorized users.

H. Park (✉)
Department of Bioscience and Biotechnology, Sejong University, 98 Kunja-Dong, Kwangjin-Ku, Seoul 143-747, Korea
e-mail: hspark@sejong.ac.kr

S. Hong · S. Hong (✉)
Department of Chemistry, Korea Advanced Institute of Science and Technology (KAIST), Taejon 305-701, Korea
e-mail: hongorg@kaist.ac.kr

Introduction

The appearance of Philadelphia chromosome is characteristic of chronic myelogenous leukemia (CML), which is constructed as a result of the reciprocal translocation between Abelson (ABL) gene on chromosome 9 and breakpoint cluster region (BCR) gene on chromosome 22. This recombination of two genes leads to the production of BCR-ABL fusion protein that is a constitutively active tyrosine kinase and well known to be responsible for the pathogenesis of CML [1]. Indeed, BCR-ABL has been observed in most cases of CML as well as in some cases of acute lymphoblastic leukemia (AML). Therefore, the effective inhibition of BCR-ABL activity has been considered a novel strategy for the development of therapeutics for CML [2]. Accordingly, a great deal of efforts has been devoted to the discovery of small-molecule inhibitors of BCR-ABL, as recently reviewed in a comprehensive fashion [3]. The knowledge of a critical role of BCR-ABL in the pathogenesis of CML has thus made it possible to identify the first generation BCR-ABL inhibitors including imatinib that was approved for the clinical treatment of CML [4].

However, various mutations in the kinase domain of BCR-ABL have been shown to impede effective inhibitor binding and thereby to cause CML cells to be resistant to the first generation inhibitor drugs. Until recently, at least 100 different point mutations have been identified in CML patients who have resistance to imatinib [5]. The emergence of such a drug resistance has prevented the first generation anti-CML drugs from being used in clinical treatment, which triggered the development of the new BCR-ABL inhibitors that can also be a potent inhibitor of the imatinib-resistant mutants [6]. These second-generation inhibitors include dasatinib [7], nilotinib [8], bafetib [9], bosutinib [10], PPY-A [11], tozasertib [12], danusertib [13], AT-9283 [14], and KW-2449 [15]. Among the drug-resistant variants, T315I mutant has been most difficult to be deactivated with ATP-competitive BCR-ABL inhibitors because the mutation at the gatekeeper site (residue 315) can not only alter the geometry of ATP-binding pocket but also eliminate a critical hydrogen bond required for tight binding of the inhibitors [16]. However, the abundance of structural information about the nature of the interactions between BCR-ABL and small-molecule inhibitors for the wild type and the mutants has made it a plausible task to discover a good lead compound for new anti-CML drugs. Indeed, some common inhibitors of wild type and T315I mutant of BCR-ABL were also discovered on the basis of such structural information [17–21].

Although most of the known inhibitors were discovered with high-throughput screening of chemical libraries and some structural modifications of the existing inhibitor scaffolds, some rational design approaches using docking simulations in the ATP-binding site of BCR-ABL have also been applied to explain the observed inhibitory activities [22–24]. In the present study, we aim to identify the common inhibitors of the wild type and T315I mutant of BCR-ABL by means of the parallel virtual screening approaches with docking simulations of probe molecules in the ATP-binding sites of the wild type and the mutant. Virtual screening has not always been successful due to the inaccuracy in the scoring function, which leads to a weak correlation between the computational predictions and experimental results for binding affinities [25]. The characteristic feature that discriminates our virtual screening approach from the others lies in the implementation of an accurate solvation model in calculating the binding free energies between BCR-ABL and the putative ligands, which would have an effect of increasing the accuracy of the scoring function in a docking program [26]. It is shown in this study that the docking simulations with the improved binding free energy function can be useful for enriching the chemical library with molecules that are likely to have inhibitory activities against the wild-type and T315I mutant of BCR-ABL, as well as for elucidating the activities of the identified inhibitors.

Computational methods

We prepared the two receptor models from the X-ray crystal structure of the wild-type BCR-ABL in complex with imatinib (PDB code: 1IEP) [27] and that of T315I mutant in complex with AP24535 (PDB code: 3IK3) [28] to perform the parallel virtual screening with docking simulations for the identification of the common inhibitors in a chemical database. To obtain the all-atom models for the receptors, hydrogen atoms were added to each protein atom in the wild type and mutant enzymes. A special attention was paid to assign the protonation states of the ionizable Asp, Glu, His, and Lys residues in the X-ray crystal structures of the wild type and T315I mutant. The side chains of Asp and Glu residues were assumed to be neutral if one of their carboxylate oxygens pointed toward a hydrogen-bond accepting group including the backbone aminocarbonyl oxygen at a distance within 3.5 Å, a generally accepted distance limit for a hydrogen bond of moderate strength [29]. Similarly, the lysine side chains were assumed to be protonated unless the NZ atom was in proximity to a hydrogen-bond donating group. The same procedure was also applied to determine the protonation states of ND and NE atoms in His residues.

The docking library for the wild type and T315I mutant of BCR-ABL comprising about 240,000 compounds was constructed from the latest version of the chemical database distributed by Interbioscreen (http://www.ibscreen.com) containing approximately 477,000 synthetic and natural compounds. Prior to the virtual screening with docking simulations, they were filtrated on the basis of Lipinski's "Rule of Five" to adopt only the compounds with the physicochemical properties of potential drug candidates [30] and without reactive functional group(s). To remove the structural redundancies in the chemical library, structurally similar compounds with a Tanimoto coefficient exceeding 0.85 were clustered into a single representative molecule. Molecular similarities were measured using the fingerprints of each molecule, generated using the Daylight software as an ASCII string of 1s and 0s. All of the compounds included in the docking library were then processed by the Corina program to generate their 3D atomic coordinates, followed by the assignment of Gasteiger-Marsilli atomic charges [31]. We used the AutoDock program [32] in virtual screening of the inhibitors for the wild type and T315I mutant of BCR-BAL because the outperformance of its scoring function over those of the others had been shown in several target proteins [33]. AMBER force field parameters were assigned for calculating the van der Waals interactions and the internal energy of a ligand as implemented in the original AutoDock program. Two parallel virtual screening processes with docking simulations were then carried out to

identify the common inhibitors equipotent for the wild type and T315I mutant of BCR-ABL.

In the actual docking simulations for virtual screening, we used the empirical AutoDock scoring function improved by the implementation of a new solvation model for a compound. The modified scoring function has the following form:

$$\Delta G_{bind}^{aq} = W_{vdW}\sum_{i=1}\sum_{j=1}\left(\frac{A_{ij}}{r_{ij}^{12}}-\frac{B_{ij}}{r_{ij}^{6}}\right) + W_{hbond}\sum_{i=1}\sum_{j=1}E(t).\times\left(\frac{C_{ij}}{r_{ij}^{12}}-\frac{D_{ij}}{r_{ij}^{10}}\right) + W_{elec}\sum_{i=1}\sum_{j=1}\frac{q_i q_j}{\varepsilon(r_{ij})r_{ij}} + W_{tor}N_{tor} + W_{sol}\sum_{i=1}S_i\left(Occ_i^{\max}-\sum_{j>i}V_j e^{-\frac{r_{ij}^2}{2\sigma^2}}\right), \quad (1)$$

where W_{vdW}, W_{hbond}, W_{elec}, W_{tor}, and W_{sol} are the weighting factors of van der Waals, hydrogen bond, electrostatic interactions, torsional term, and desolvation energy of an inhibitor, respectively. r_{ij} represents the interatomic distance, and A_{ij}, B_{ij}, C_{ij}, and D_{ij} are related to the depths of the potential energy well and the equilibrium separations between the two atoms. The hydrogen bond term has an additional weighting factor, $E(t)$, representing the angle-dependent directionality. Cubic equation approach was applied to obtain the dielectric constant required in computing the interatomic electrostatic interactions between BCR-ABL and a ligand molecule [34]. In the entropic term, N_{tor} is the number of all rotatable bonds in the ligand. In the desolvation term, S_i and V_i are the solvation parameter and the fragmental volume of atom i [35], respectively, while $Occ_i^{\max}$ stands for the maximum atomic occupancy. In the calculation of molecular solvation free energy term in Eq. **1**, we used the atomic parameters developed by Kang et al. [36] because those of the atoms other than carbon were unavailable in the current version of the AutoDock program. This modification of the solvation free energy term is expected to increase the accuracy in virtual screening because the underestimation of ligand solvation often leads to the overestimation of the binding affinity of a ligand with many polar atoms [26]. Indeed, the superiority of this modified scoring function to the previous one was well-appreciated in recent studies for virtual screening of kinase and phosphatase inhibitors [37, 38].

The docking simulation of a compound in the docking library started with 3D grid calculations of the interaction energies given by all the possible atom types for all compounds under investigation. These uniquely defined potential grids for the receptor protein were then used in common for docking simulations of all compounds in the docking library. As the center of the common grids, we used the center of mass coordinates of imatinib [27] and AP24534 [28] bound in the ATP-binding sites of the wild type and T315I mutant of BCR-ABL, respectively. The calculated grid maps were of dimension 61 × 61 × 61 points with the spacing of 0.375 Å, yielding a receptor model that includes atoms within 22.9 Å of the grid center. For each compound in the docking library, 10 docking runs were performed with the initial population of 50 individuals. Maximum number of generations and energy evaluation were set to 27,000 and 2.5×10^5, respectively. Docking simulations with the improved scoring function were then carried out in the ATP-binding sites of the wild type and T315I mutant of BCR-ABL to score and rank the compounds in the docking library according to the calculated binding free energies for the two independent target proteins.

Results and discussion

At first we performed the test calculations for validation of virtual screening with the improved scoring function. The test set of compounds for docking simulations with respect to T315I mutant of BCR-ABL comprises 20 known inhibitors and 980 compounds selected at random from InterBioScreen database. The structures of 20 known inhibitors are shown in Supplementary Material. Then, we compared the performances of the improved and the original scoring functions in virtual screening of T315I mutant inhibitors. Compared in Fig. 1 are the percentages of true hits retrieved by the improved and the original scoring functions in various top-scoring fractions of database selected for generating a hit list. We note that the improved scoring function performs better than the previous one in providing the highest enrichment at every fraction cutoff. For example, the former picks four actives seeded in top 1 % of the database as compared to only two

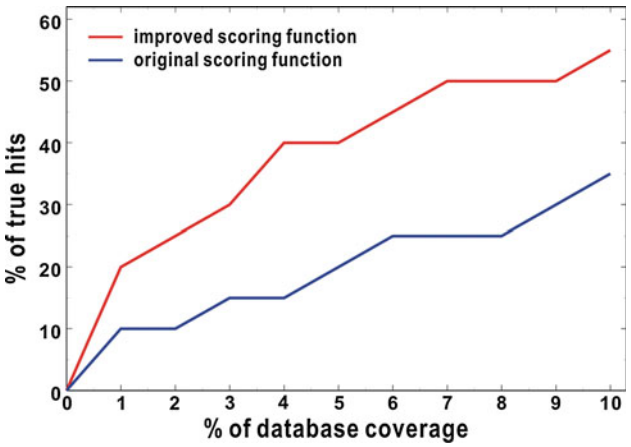

Fig. 1 The cumulative percentage of known inhibitors of T315I mutant of BCR-ABL recovered by virtual screening as a function of the top-scoring fraction of database selected for generating a hit list

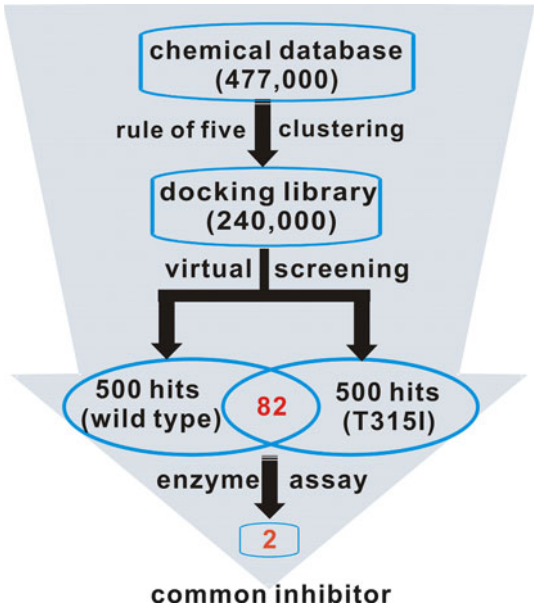

Fig. 2 Flowchart for the discovery of common inhibitors of the wild type and T315I mutant of BCR-ABL through the two parallel virtual screening and enzyme assay processes

for the latter. The outperformance of the improved scoring function becomes clearer when one compares the abilities to pick out the most actives out of a cumulative total of the twenty known inhibitors seeded in the test set. When 10 % of the database is considered, for example, the improved scoring function retrieved a total of eleven actives out of total 20, as compared to only seven actives by the previous one. Thus, the outperformance of the improved scoring function reveals a consistency for all cutoffs, and indicates its superiority over the original one in predicting the binding free energies of putative T315I mutant inhibitors. It is apparent that such an enhancement in the efficiency of virtual screening can be attributed to the incorporation of ligand solvation effects in the scoring function.

A total of 240,000 compounds were screened with docking simulations with respect to the wild type and T315 mutant of BCR-ABL to select 500 top-scored compounds as virtual hits for each of the two targets. The two hit sets included 82 compounds in common as depicted in Fig. 2, which were purchased from the compound supplier (Interbioscreen Ltd.). As a check on the validity of the present virtual screening procedure, we compared the binding free energies of the twenty known dual inhibitors for the wild type and T315I mutant of BCR-ABL with those of the compounds in the docking library. Four of them (dasatinib, danusertib, compound **2** in Ref. [17], and compound **4** in Ref. [20]) were found to belong to 500 top-scored virtual hits for both the wild type and T315I mutant. These validation results exemplify the reliability of the present computational strategy to identify the common inhibitors. The 82 putative common inhibitors were then tested over the wild type and T315I mutant at 50 μM concentration in a high-throughput binding assay (KINOMEscan, Ambit Biosciences) [39], using the broad kinase inhibitor staurosporine as the reference. As a consequence of the two parallel virtual screening and enzyme assay processes, two compounds were identified as the common inhibitors of the wild type and T315I mutant of BCR-ABL. Both inhibitors exhibited a high potency for the wild type and T315I mutant with percent of control (POC) values less than 25, and were selected to determine the IC_{50} values.

The chemical structures and the inhibitory activities of the identified common inhibitors against the wild type and T315I mutant are shown in Fig. 3 and Table 1, respectively. It is a common structural feature for **1** and **2** that multiple hydrogen bonding groups flank the nonpolar aromatic rings that reside at both ends of the molecular structure. This indicates that both hydrogen-bond and hydrophobic interactions should be the significant binding forces to stabilize the inhibitors in the ATP-binding sites. To the best of our knowledge, neither **1** nor **2** has been reported as BCR-ABL inhibitors so far. We also checked the structural similarity of **1** and **2** to the known BCR-ABL inhibitors in the two most public chemical databases, ChEMBL and PubChem. However, none of BCR-ABL inhibitors in the databases were found to include 2-(5-hydroxy-2-methyl-4-oxo-4*H*-chromen-7-yloxy)-*N*-pyridin-2-yl-acetamide or benzofuran-2-carboxylic acid amide moiety in their chemical structures, which are the key structural elements of **1** and **2**, respectively. As can be seen in Table 1, **1** and **2** reveal a high inhibitory activity against both the wild type and T315I mutant of BCR-ABL with the IC_{50} values ranging from 3 to 10 μM. Because the two inhibitors are structurally different and were screened for having good physicochemical properties as a drug candidate, both deserve consideration for further development by structure–activity relationship (SAR) studies to optimize the inhibitory activities to develop a new anti-CML medicine. Although the inhibitory activity of **2** is lower than **1** by a factor of 3 for both the wild type and the mutant, it is nonetheless expected to serve as a new inhibitor scaffold from which much more potent inhibitors can be derivatized due to the low molecular weight (318).

To obtain some structural insight into the inhibitory mechanisms for the identified common inhibitors of the wild type and T315I mutant of BCR-ABL, their binding modes in the ATP-binding sites were investigated in a comparative fashion. Figure 4 shows the lowest-energy conformations of **1** and **2** in the ATP-binding sites of the wild type and T315I mutant calculated with the modified AutoDock scoring function. We note that the binding modes of **1** and **2** for the wild type are completely different from those for T315I mutant. As the amino acid changes

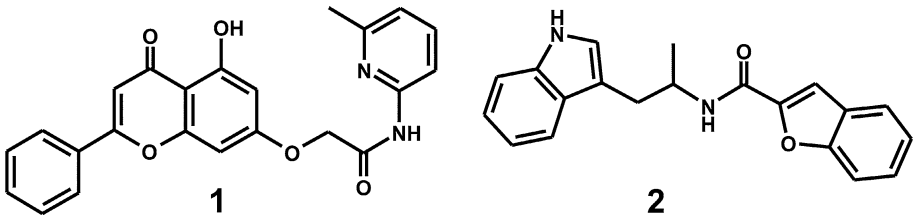

Fig. 3 Chemical structures of the identified common inhibitors for the wild type and T315I mutant of BCR-ABL

Table 1 POC and IC_{50} (in μM) values of the two identified common inhibitors against the wild type and T315I mutant of BCR-ABL

Inhibitor	POC		IC_{50}	
	Wild type	T315I mutant	Wild type	T315I mutant
1	14	6.6	3.3	2.7
2	22	14	10.6	9.7

from Thr to Ile at residue 315, for example, **1** appears to move away from the entrance of the ATP-binding site (Fig. 4A) to the two α-helices residing at the N- and C-terminal domains (Fig. 4B) with the positions of its terminal pyridine and phenyl rings being reversed. A similar positional shift is also observed in the calculated binding modes of **2**. It moves to the space between the two α-helices in the T315I-**2** complex (Fig. 4B) and exchanges the positions of its terminal indole and benzofuran rings in comparison to the binding mode in the BCR-ABL-**2** complex (Fig. 4A) in which a large part of **2** resides at the end of the ATP-binding site. As indicated in Fig. 4, the weakening of the interactions of **1** and **2** with the ATP-binding site should be attributed to the increase in van der Waals volume at residue 315 due to the substitution of Ile for Thr and the resulting increase in repulsive interactions between protein and ligand groups in the ATP-binding site. As a check on the presence of another stable binding modes, we carried out additional docking simulations of **1** and **2** in an extensive fashion with varying docking parameters. It is found from clustering analysis of the results for total 100 docking runs that the binding modes shown in Fig. 4 represent the lowest-energy cluster with 75, 72, 62, and 76 % of total population for the calculated BCR-ABL-**1**, BCR-ABL-**2**, T315I-**1**, and T315I-**2** complexes, respectively. These results confirm that the binding modes of **1** and **2** for T315I mutant differ from those for the wild type due to the increase in the repulsive interactions between residue 315 and the central hydrophilic portion of the inhibitors. In turn, such a substantial difference in the binding modes can be invoked to explain the difficulty in designing the common inhibitors that can be equipotent for both the wild type and T315I mutant of BCR-ABL.

Although most of the BCR-ABL inhibitors available today are ATP-competitive, some inhibitors are known to have a different mode of action to impair the kinase activity of BCR-ABL by binding to a site remote from the ATP-binding pocket. These allosteric inhibitors proved to be able to exhibit a promising therapeutic activity in the context of overcoming the clinically acquired resistance to the first generation anti-CML drugs [40]. In order to examine the possibility of the allosteric inhibition of the wild type and T315I mutant by the two identified inhibitors, therefore, docking simulations were carried out with the grid maps for the two receptor models so as to include the entire part of the kinase domain although no binding pocket in the outer region of BCR-ABL had been identified yet. However, a binding configuration in which the newly identified inhibitors reside outside the ATP-binding site was observed neither for the wild type nor for the mutant. This result supports the possibility that **1** and **2** would impair the kinase activity of the wild type and T315I mutant of BCR-ABL through the specific binding in their respective ATP-binding sites.

The calculated binding modes of the inhibitor **1** in the ATP-binding sites of the wild type and T315I mutant are compared in Fig. 5. It is seen that the inhibitor interacts with the wild type and the mutant in a completely different way due most probably to the difference in amino acid residue at position 315 that is a component of the ATP-binding site. Consistent with the general structural feature in the interactions between the wild-type BCR-ABL and its potent inhibitors, the side-chain hydroxyl moiety of Thr315 appears to play a significant role in stabilizing **1** in the ATP-binding site by donating a hydrogen bond to the carbonyl group of the inhibitor (Fig. 5A). The central phenolic group of **1** receives and donates a hydrogen bond from the backbone amidic nitrogen of Met318 and to the backbone aminocarbonyl oxygen of Glu316, respectively. These hydrogen bonds seem to play a role of anchoring **1** at the ATP-binding site because they are established in the middle of the binding pocket. The 5-hydroxy-cromen-4-one group of **1** can thus form three hydrogen bonds at the ATP-binding site, which indicates that it should be a key structural element that can be considered in designing new inhibitors of BCR-ABL. A stable hydrogen bond is also established at the entrance of ATP-binding site between the inhibitor amidic nitrogen and the backbone aminocarbonyl oxygen of Met318. The hydrogen-bond stabilization of the inhibitors by backbone groups of Met318 was also observed in the X-ray crystal structures of BCR-ABL in complex with the potent inhibitors [27]. This consistency

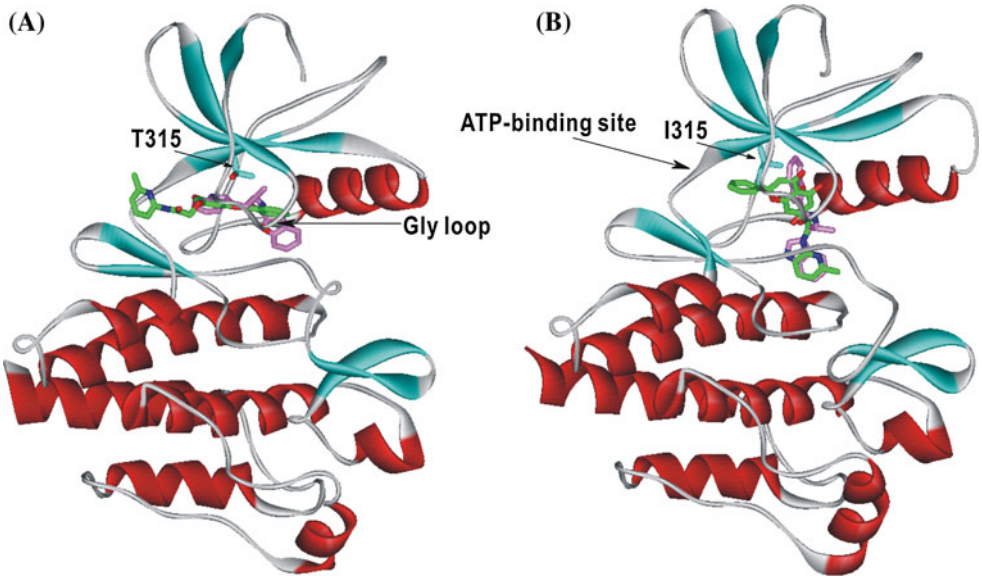

Fig. 4 Comparative view of the binding modes of the BCR-ABL inhibitors in the ATP binding sites of (**A**) wild type and (**B**) T315I mutant. Carbon atoms of **1** and **2** are indicated in *green* and *pink*, respectively. The side chains of residue 315 are also indicated

supports the reasonableness of the binding mode of **1** calculated with the modified scoring function. The inhibitor **1** can be further stabilized in the ATP-binding site of BCR-ABL by the hydrophobic interactions of its nonpolor groups with the side chains of Leu248, Tyr253, Val256, Ala269, Val299, Phe317, Leu370, and Phe382. Thus, the overall structural features derived from docking simulations indicates that the micromolar inhibitory activity of **1** against the wild type of BCR-ABL should stem from the multiple hydrogen bonds and hydrophobic interactions established simultaneously in the ATP-binding site.

We note that **1** is bound in the ATP-binding site of T315I mutant in the opposite direction to its binding mode for the wild type, which is in contrast to the results for some known inhibitors of T315I that were shown to bind in the ATP-binding site of the wild-type and the mutant in a similar fashion [11, 28]. Such a difference in the inhibition mechanisms is actually not surprising because **1** is structurally very different from the exiting ones. In the calculated T315I-**1** complex, the role of hydrogen bond acceptor with respect to the inhibitor phenolic group is played by the side-chain carboxylate ion of Glu286 (Fig. 5B) instead of a backbone aminocarbonyl group. An additional hydrogen bond appears to be formed between the etheric oxygen of **1** and the backbone amidic nitrogen of Asp381, which should also be a significant binding force to stabilize **1** in the ATP-binding site of T315I mutant. However, it is noteworthy that the number of hydrogen bonds decreases from four in BCR-ABL-**1** to two in T315I-**1** complex, which has an effect of lowering the binding affinity. On the other hand, at least eight additional nonpolar residues (Met290, Ile293, Leu298, Ile315, Leu354, His361, Val379, and Ala380) were observed at the interface of van der Waals contacts between **1** and T315I mutant of BCR-ABL. Consistent with

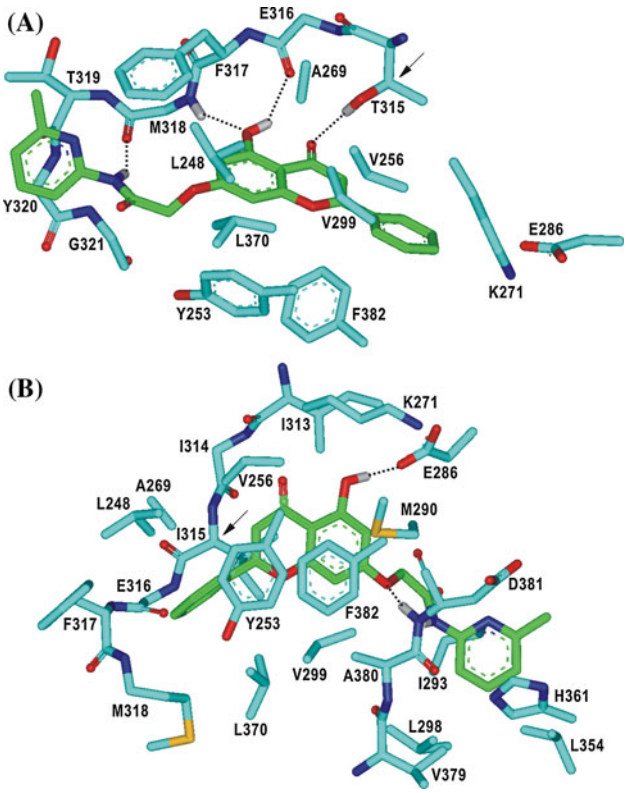

Fig. 5 Calculated binding modes of **1** in the ATP-binding sites of (**A**) wild type and (**B**) T315I mutant of BCR-ABL. Carbon atoms of the protein and the ligand are indicated in *cyan* and *green*, respectively. Each *dotted line* indicates a hydrogen bond

these changes in binding modes, the hydrophilic interactions (electrostatic plus hydrogen bond) are found to become less favorable from −21.7 kcal in BCR-ABL-**1** complex to −20.8 kcal/mol in T315I-**1** complex as compared to the decrease in van der Waals interaction energy

values from −8.6 to −10.2 kcal/mol. Thus, the structural and energetic features found in docking simulations indicate that the hydrophobic interactions of **1** with T315I mutant should be even stronger than those with the wild type. Such a significant strengthening of hydrophobic interactions seems to be sufficient to compensate for the weakening of the hydrogen bond interactions with the change of the receptor from the wild type to T315I mutant, which can be invoked to explain a little higher inhibitory activity of **1** for the mutant than for the wild type (Table 1).

The inhibitor **2** exhibited also a little higher inhibitory activity against T315I mutant than the wild type. Its binding modes in the ATP-binding sites of the wild type and the mutant are compared in Fig. 6. As in the BCR-ABL-**1** complex, the side-chain hydroxyl moiety of Thr315 donates a hydrogen bond to the carbonyl oxygen of **2** (Fig. 6A), which confirms its important role in binding of the inhibitors in the ATP-binding site of the wild-type BCR-ABL. An additional hydrogen bond is established between the backbone aminocarbonyl oxygen of Glu316 and the indole moiety of **2**. The hydrogen-bond interactions in the BCR-ABL-**2** complex are thus likely to be weaker than those in the BCR-ABL-**1** complex in which four hydrogen bonds are involved (Fig. 5A). On the other hand, the nonpolar aromatic rings of **2** in the BCR-ABL-**2** complex are stabilized in a similar fashion to those of **1** in the BCR-ABL-**1** complex: its indole and benzofuran rings form the van der Waals contacts with the hydrophobic side chains of Leu248, Tyr253, Val256, Ala269, Met290, Val299, Met318, Leu370, Ala380, and Phe382. Therefore, the weakening of the hydrogen-bond interactions in going from BCR-ABL-**1** to BCR-ABL-**2** complex may be invoked to explain the more than three-fold lower potency of **2** than **1** with respect to the wild type (Table 1).

As the receptor changes from the wild type to T315I mutant, the binding mode of **2** is found to undergo a similar change to that of **1**. For example, the calculated T315I-**2** complex appears to involve only one hydrogen bond established between the aminocarbonyl oxygen of **2** and the backbone amidic nitrogen of Asp381 (Fig. 6B) as compared to the presence of two hydrogen bonds in the BCR-ABL-**2** complex. In order for **2** to be a common inhibitor for the wild type and the mutant, therefore, the strengthening of van der Waals interactions should be necessary for the tight binding of **2** in the ATP-binding site of T315I mutant to compensate for the weakening of hydrogen bond interactions. We note in this regard that when compared to the BCR-ABL-**2** complex, at least two more nonpolar residues are observed at the interface of van der Waals contact in the T315I-**2** complex in which the indole and benzofuran rings of **2** are stabilized in the hydrophobic pockets comprising the side chains of Val256, Ala269, Val289, Met290, Leu298, Val299, Ile315, Leu354,

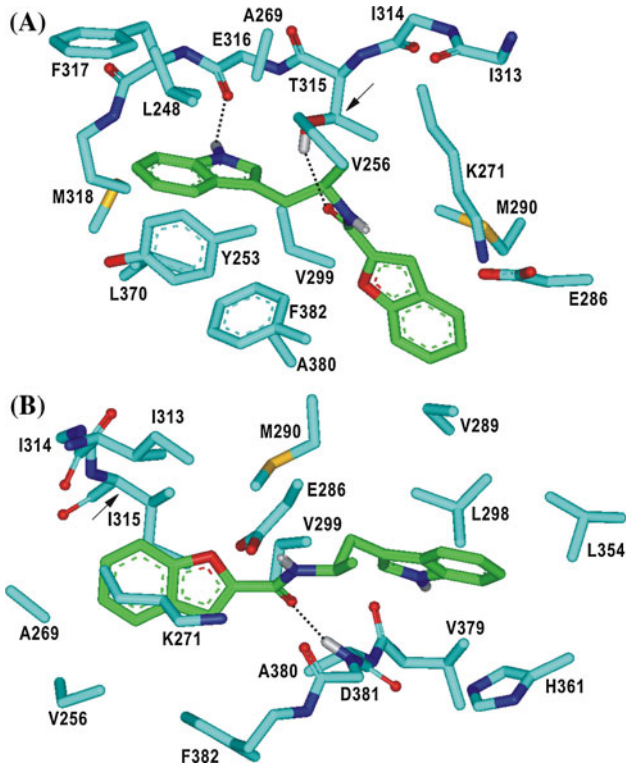

Fig. 6 Calculated binding modes of **2** in the ATP-binding sites of (**A**) wild type and (**B**) T315I mutant of BCR-ABL. Carbon atoms of the protein and the ligand are indicated in *cyan* and *green*, respectively. Each *dotted line* indicates a hydrogen bond

His361, Val379, Ala380, and Phe382. Furthermore, it is also noteworthy that both terminal nonpolar groups of **2** are accommodated in the hydrophobic pockets in the T315I-**2** complex whereas one side of the benzofuran ring is exposed to bulk solvent in the BCR-ABL-**2** complex. These differences in binding modes of **2** for the wild type and the mutant are consistent with the decrease in van der Waals interaction energy values from −7.1 kcal/mol in BCR-ABL-**2** complex to −8.9 kcal/mol in T315I-**2** complex in contrast to the increase in hydrophilic interactions energy values from −20.2 to −19.0 kcal/mol. The strengthening of hydrophobic interactions in the T315I-**2** complex is thus most likely to make the inhibitor **2** more potent for the mutant than for the wild type by effectively overcoming the structural disadvantage for forming the hydrogen bonds in the ATP-binding site. Because this is the common differential inhibitory mechanism for **1** and **2**, it can be argued that the ability to switching the major binding forces from hydrogen bonds to van der Waals interactions should be necessary for the simultaneous inhibition of the wild type and T315I mutant of BCR-ABL.

We finally examine if the hypothesis on the differential inhibitory mechanisms for the wild type and T315I mutant can explain the experimental SAR results of the known

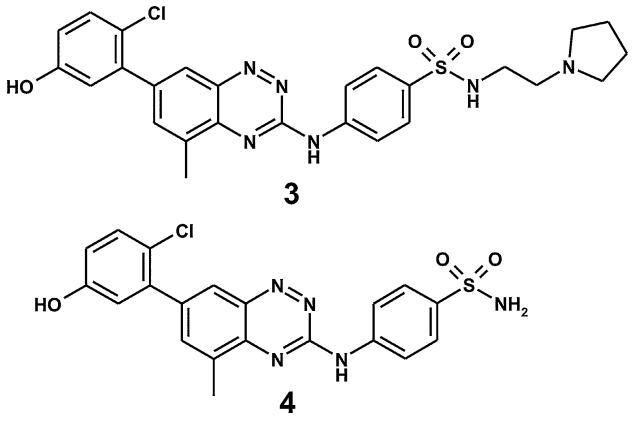

Fig. 7 Chemical structures of the two BCR-ABL inhibitors selected in docking analysis

BCR-ABL inhibitors. Two compounds in Ref. 21 (**3** and **4** Fig. 7) were selected in this validation study, which differ only by the presence or absence of the ethylpyrrolidine group at the end of molecular structure.

It was known that the K_i value for T315I mutant of BCR-ABL increased substantially from 3.4 to 687 nM with the change of the terminal ethylpyrrolidine moiety in **3** to hydrogen in **4** whereas those of the two inhibitors with respect to the wild type BCR-ABL were quite similar (3.0 for **3** and 7.7 nM for **4**).[21] As an effort to elucidate these different SAR results, we carried out docking simulations of **3** and **4** in the ATP-binding sites of the wild type and T315I mutant. Figure 8 shows the calculated binding modes of the two inhibitors with respect to the wild type and the mutant. The two inhibitors appear to be bound in the ATP-binding site of wild type in the same fashion with the establishment of two hydrogen bonds with the side chains of Tyr253 and Thr315 (Fig. 8A). Apparently, these two hydrogen bonds should be the most significant binding forces for stabilizing both BCR-ABL-inhibitor complexes of the wild type. It is also noteworthy that only two hydrophobic residues (Met290 and Val299) are found within 5 Å of the terminal ethylpyrrolidine group of **3** that resides at the bottom of the N-terminal domain and points toward bulk solvent. The similar inhibitory activities of **3** and **4** against the wild-type BCR-ABL can thus be attributed to the weak hydrophobic interactions of the terminal ethylpyrrolidine moiety of **3** with its nonpolar amino acids.

As can be seen in Fig. 8B, only one hydrogen bond involving the inhibitor sulfonamide group seems to play a role in stabilizing the T315I mutant in complex with **3** and **4** in which much more nonpolar residues are observed at the protein–ligand interfaces than in the BCR-ABL-inhibitor complexes of the wild type. In particular, it is noteworthy that the terminal ethylpyrrolidine group of **3** is fully accommodated in a hydrophobic pocket comprising the side chains of Val256, Ala269, Met290, Val299, Ile313,

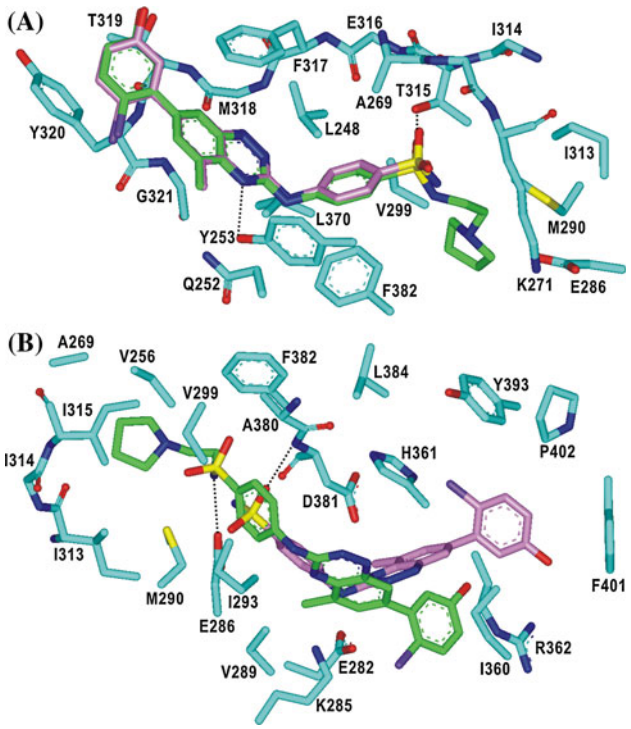

Fig. 8 Calculated binding modes of **3** and **4** in the ATP-binding sites of (**A**) wild type and (**B**) T315I mutant of BCR-ABL. Carbon atoms of the protein, **3**, and **4** are indicated in *cyan*, *green*, and *pink*, respectively. Each *dotted line* indicates a hydrogen bond

and Ile315. It is actually impossible for such a stable van der Waals contact to be established in T315I-**4** complex, which should be responsible for the 200-fold decrease in inhibitory activity in going from **3** to **4**. Thus, the difference in binding modes of **3** between the wild type and the mutant confirms that in order for a BCR-ABL inhibitor to be equipotent to T315I mutant, it should be capable of compensating for the loss of a hydrogen bond with Thr315 by strengthening the hydrophobic interactions with nonpolar residues including Ile315 in complexation with the mutant.

Conclusions

We have identified two novel common inhibitors of the wild type and T315I mutant of BCR-ABL by applying a computer-aided drug design protocol involving the structure-based virtual screening with docking simulations. These inhibitors were screened for having desirable physicochemical properties as a drug candidate and revealed micromolar inhibitory activities. Therefore, both of the common inhibitors may serve as a new starting point for further SAR studies to optimize the inhibitory activities simultaneously against the wild type and the mutant. Detailed binding mode analyses with docking simulations

showed that both inhibitors could be stabilized in the ATP-binding site of the wild type by the establishment of multiple hydrogen bonds and van der Waals contacts in a cooperative fashion. The hydrogen bond interactions appeared to get weaker with the change of the receptor from the wild type to T315I mutant due to the disappearance of the hydroxy group in the ATP-binding site. However, the common inhibitors were found to maintain the inhibitory activity against the mutant by changing the binding mode in such a way to maximize the hydrophobic interactions in the ATP-binding site. It can thus be argued that in order for a BCR-ABL inhibitor to be also potent against T315I mutant, it should be capable of compensating for the loss of hydrogen bonds by strengthening the van der Waals interactions in the ATP-binding site. These differential binding modes may serve as a key feature that should be kept in mind in designing the new inhibitors equipotent for the wild type and T315I mutant of BCR-ABL.

Acknowledgments We could perform this study with the financial support by Basic Science Research Program through National Research Foundation of Korea (NRF) funded by Ministry of Education, Science and Technology (2011-0022858). This research was also supported by NRF funded by Ministry of Education, Science and Technology (NRF-2011-2011-0026680, 2011-0016436 and 2011-0020322).

References

1. Quintas-Cardama A, Cortes J (2009) Molecular biology of *bcr-abl1*-positive chronic myeloid leukemia. Blood 113:1619–1630
2. Eck MJ, Manley PW (2009) The interplay of structural information and functional studies in kinase drug design: insights from BCR-Abl. Curr Opin Cell Biol 21:288–295
3. Schenone S, Bruno O, Radi M, Botta M (2010) New insights into small-molecule inhibitors of Bcr-Abl. Med Res Rev 31:1–41
4. Capdeville R, Buchdunger E, Zimmermann J, Matter A (2002) Glivec (STI571, imatinib), a rationally developed, targeted anticancer drug. Nat Rev Drug Discov 1:493–503
5. O'Hare T, Eide CA, Deininger MW (2007) Bcr-Abl kinase domain mutations, drug resistance, and the road to a cure for chronic myeloid leukemia. Blood 110:2242–2249
6. Quintas-Cardama A, Kantarjian H, Cortes J (2007) Flying under the radar: the new wave of BCR-ABL inhibitors. Nat Rev Drug Discov 6:834–848
7. Lombardo LJ, Lee FY, Chen P, Norris D, Barrish JC, Behnia K, Castaneda S, Cornelius LAM, Das J, Doweyko AM, Fairchild C, Hunt JT, Inigo I, Johnston K, Kamath A, Kan D, Klei H, Marathe P, Pang S, Peterson R, Pitt S, Schieven GL, Schmidt RJ, Tokarski J, Wen ML, Wityak J, Borzilleri RM (2004) Discovery of *N*-(2-chloro-6-methyl- phenyl)-2-(6-(4-(2-hydroxyethyl)-piperazin-1-yl)-2-methylpyrimidin-4-ylamino)thiazole-5-carboxamide (BMS-354825), a dual Src/Abl kinase inhibitor with potent antitumor activity in preclinical assays. J Med Chem 47:6658–6661
8. Weisberg E, Manley PW, Breitenstein W, Brüggen J, Cowan-Jacob SW, Ray A, Huntly B, Fabbro D, Fendrich G, Hall-Meyers E, Kung AL, Mestan J, Daley GQ, Callahan L, Catley L, Cavazza C, Azam M, Neuberg D, Wright RD, Gilliland DG, Griffin JD (2005) Characterization of AMN107, a selective inhibitor of native and mutant Bcr-Abl. Cancer Cell 7:129–141
9. Kimura S, Naito H, Segawa H, Kuroda J, Yuasa T, Sato K, Yokota A, Kamitsuji Y, Kawata E, Ashihara E, Nakaya Y, Naruoka H, Wakayama T, Nasu K, Asaki T, Niwa T, Hirabayashi K, Maekawa T (2005) NS-187, a potent and selective dual Bcr-Abl/Lyn tyrosine kinase inhibitor, is a novel agent for imatinib-resistant leukemia. Blood 106:3948–3954
10. Boschelli DH, Ye F, Wang YD, Dutia M, Johnson SL, Wu B, Miller K, Powell DW, Yaczko D, Young M, Tischler M, Arndt K, Discafani C, Etienne C, Gibbons J, Grod J, Lucas J, Weber JM, Boschelli F (2001) Optimization of 4-phenylamino-3-quinolinecarbonitriles as potent inhibitors of Src kinase activity. J Med Chem 44:3965–3977
11. Zhou T, Parillon L, Li F, Wang Y, Keats J, Lamore S, Xu Q, Shakespeare W, Dalgarno D, Zhu X (2007) Crystal structure of the T315I mutant of Abl kinase. Chem Biol Drug Des 70: 171–181
12. Giles FJ, Cortes J, Jones D, Bergstrom D, Kantarjian H, Freedman SJ (2007) MK-0457, a novel kinase inhibitor, is active in patients with chronic myeloid leukemia or acute lymphocytic leukemia with the T315I BCR-ABL mutation. Blood 109:500–502
13. Gontarewicz A, Balabanov S, Keller G, Colombo R, Graziano A, Pesenti E, Benten D, Bokemeyer C, Fiedler W, Moll J, Brümmendorf TH (2008) Simultaneous targeting of Aurora kinases and Bcr-Abl kinase by the small molecule inhibitor PHA-739358 is effective against imatinib-resistant BCR-ABL mutations including T315I. Blood 111:4355–4364
14. Howard S, Berdini V, Boulstridge JA, Carr MG, Cross DM, Curry J, Devine LA, Early TR, Fazal L, Gill AL, Heathcote M, Maman S, Matthews JE, McMenamin RL, Navarro EF, O'Brien MA, O'Reilly M, Rees DC, Reule M, Tisi D, Williams G, Vinković M, Wyatt PG (2009) Fragment-based discovery of the pyrazol-4-yl urea (AT9283), a multitargeted kinase inhibitor with potent aurora kinase activity. J Med Chem 52:379–388
15. Shiotsu Y, Kiyoi H, Ishikawa Y, Tanizaki R, Shimizu M, Umehara H, Ishii K, Mori Y, Ozeki K, Minami Y, Abe A, Maeda H, Akiyama T, Kanda Y, Sato Y, Akinaga S, Naoe T (2009) KW-2449, a novel multikinase inhibitor, suppresses the growth of leukemia cells with FLT3 mutations or T315I-mutated BCR/ABL translocation. Blood 114:1607–1617
16. Quintas-Cardama A, Cortes J (2008) Therapeutic options against BCR-ABL1 T315I positive chronic myelogenous leukemia. Clin Cancer Res 14:4392–4399
17. Choi HG, Ren P, Adrian F, Sun F, Lee HS, Wang X, Ding Q, Zhang G, Xie Y, Zhang J, Liu Y, Tuntland T, Warmuth M, Manley PW, Mestan J, Gray NS, Sim T (2010) A type-II kinase inhibitor capable of inhibiting the T315I "gatekeeper" mutant of Bcr-Abl. J Med Chem 53:5439–5448
18. Huang WS, Metcalf CA, Sundaramoorthi R, Wang Y, Zou D, Thomas RM, Zhu X, Cai L, Wen D, Liu S, Romero J, Qi J, Chen I, Banda G, Lentini SP, Das S, Xu Q, Keats J, Wang F, Wardwell S, Ning Y, Snodgrass JT, Broudy MI, Russian K, Zhou T, Commodore L, Narasimhan NI, Mohemmad QK, Iuliucci J, Rivera VM, Dalgarno DC, Sawyer TK, Clackson T, Shakespeare WC (2010) Discovery of 3-[2-(imidazo[1,2-*b*]pyridazin-3-yl)ethynyl]-4-methyl-*N*-{4-[(4-methylpiperazin-1-yl)methyl]-3-(trifluoromethyl)phenyl}benzamide (AP24534), a potent, orally active pan-inhibitor of breakpoint cluster region-abelson (BCR-ABL) kinase including the T315I gatekeeper mutant. J Med Chem 53:4701–4719
19. Thomas M, Huang WS, Wen D, Zhu X, Wang Y, Metcalf CA, Liu S, Chen I, Romero J, Zou D, Sundaramoorthi R, Li F, Qi J, Cai L, Zhou T, Commodore L, Xu Q, Keats J, Wang F, Wardwell S, Ning Y, Snodgrass JT, Broudy MI, Russian K, Iuliucci J,

Rivera VM, Sawyer TK, Dalgarno DC, Clackson T, Shakespeare WC (2011) Discovery of 5-(arenethynyl) hetero-monocyclic derivatives as potent inhibitors of BCR–ABL including the T315I gatekeeper mutant. Bioorg Med Chem Lett 21:3743–3748

20. Deng X, Lim SM, Zhang J, Gray NS (2010) Broad spectrum alkynyl inhibitors of T315I Bcr-Abl. Bioorg Med Chem Lett 20:4196–4200
21. Cao J, Fine R, Gritzen C, Hood J, Kang X, Klebansky B, Lohse D, Mak CC, McPherson A, Noronha G, Palanki MSS, Pathak VP, Renick J, Soll R, Zeng B, Zhu H (2007) The design and preliminary structure–activity relationship studies of benzotriazines as potent inhibitors of Abl and Abl-T315I enzymes. Bioorg Med Chem Lett 17:5812–5818
22. Gambacorti-Passerini C, Gasser M, Ahmed S, Assouline S, Scapozza L (2005) Abl inhibitor BMS354825 binding mode in Abelson kinase revealed by molecular docking studies. Leukemia 19:1267–1269
23. Lü S, Luo Q, Hao X, Li X, Ji L, Zheng W, Wang F (2011) Synthesis and docking study of 2-phenylaminopyrimidine Abl tyrosine kinase inhibitors. Bioorg Med Chem Lett 21:6964–6968
24. Wang D, Zhang Z, Lu X, Feng Y, Luo K, Gan J, Yingxue L, Wan J, Li X, Zhang F, Tu Z, Cai Q, Ren X, Ding K (2011) Hybrid compounds as new Bcr/Abl inhibitors. Bioorg Med Chem Lett 21:1965–1968
25. Warren GL, Andrews CW, Capelli AM, Clarke B, LaLonde J, Lambert MH, Lindvall M, Nevins N, Semus SF, Senger S, Tedesco G, Wall ID, Woolven JM, Peishoff CE, Head MS (2006) A critical assessment of docking programs and scoring functions. J Med Chem 49:5912–5931
26. Shoichet BK, Leach AR, Kuntz ID (1999) Ligand solvation in molecular docking. Proteins 34:4–16
27. Nagar B, Bornmann W, Pellicena P, Schindler T, Veach DR, Miller WT, Clarkson B, Kuriyan J (2002) Crystal structures of the kinase domain of c-Abl in complex with the small molecule inhibitors PD173955 and imatinib (STI-571). Cancer Res 62:4236–4243
28. O'Hare T, Shakespeare WC, Zhu X, Eide CA, Rivera VM, Wang F, Adrian LT, Zhou T, Huang WS, Xu Q, Metcalf CA, Tyner JW, Loriaux MM, Corbin AS, Wardwell S, Ning Y, Keats JA, Wang Y, Sundaramoorthi R, Thomas M, Zhou D, Snodgrass J, Commodore L, Sawyer TK, Dalgarno DC, Deininger MW, Druker BJ, Clackson T (2009) AP24534, a pan-BCR-ABL inhibitor for chronic myeloid leukemia, potently inhibits the T315I mutant and overcomes mutation-based resistance. Cancer Cell 16:401–412
29. Jeffrey GA (1997) An introduction to hydrogen bonding. Oxford University Press, Oxford
30. Lipinski CA, Lombardo F, Dominy BW, Feeney PJ (1997) Experimental and computational approaches to estimate solubility and permeability in drug discovery and development settings. Adv Drug Deliver Rev 23:3–25
31. Gasteiger J, Marsili M (1980) Iterative partial equalization of orbital electronegativity—a rapid access to atomic charges. Tetrahedron 36:3219–3228
32. Morris GM, Goodsell DS, Halliday RS, Huey R, Hart WE, Belew RK, Olson AJ (1998) Automated docking using a Lamarckian genetic algorithm and an empirical binding free energy function. J Comput Chem 19:1639–1662
33. Park H, Lee J, Lee S (2006) Critical assessment of the automated AutoDock as a new docking tool for virtual screening. Proteins 65:549–554
34. Park H, Jeon YH (2007) Cubic equation governing the outer-region dielectric constant of globular proteins. Phys Rev E 75:021916
35. Stouten PFW, Frömmel C, Nakamura H, Sander C (1993) An effective solvation term based on atomic occupancies for use in protein simulations. Mol Simul 10:97–120
36. Kang H, Choi H, Park H (2007) Prediction of molecular solvation free energy based on the optimization of atomic solvation parameters with genetic algorithm. J Chem Inf Model 47:509–514
37. Park H, Jeon JY, Kim SY, Jeong DG, Ryu SE (2011) Identification of novel inhibitors of mitogen-activated protein kinase phosphatase-1 with structure-based virtual screening. J Comput Aided Mol Des 25:469–475
38. Park H, Chi O, Kim J, Hong S (2011) Identification of novel inhibitors of tropomyosin-related kinase A through the structure-based virtual screening with homology-modeled protein structure. J Chem Inf Model 51:2986–2993
39. Fabian MA, Biggs WH III, Treiber DK, Atteridge CE, Azimioara MD, Bendetti MG, Carter TA, Ciceri P, Edeen PT, Floyd M, Ford JM, Galvin M, Gerlach JL, Grotzfeld RM, Herrgard S, Insko DE, Insko MA, Lai AG, Lelias JM, Mehta SA, Milanov ZV, Velasco AM, Wodicka LM, Patel HK, Zarrinkar PP, Lockhart DJ (2005) A small molecule-kinase interaction map for clinical kinase inhibitors. Nat Biotechnol 23:329–336
40. Hassan AQ, Sharma SV, Warmuth M (2010) Allosteric inhibition of BCR-ABL. Cell Cycle 9:3710–3714